SIMULATION OF CUP DRAWING BY DIFFERENT METHODS

AYAN ROY NASKAR

Department of Mechanical Engineering, National Institute of Technology, Rourkela
Rourkela, Odisha- 769008, India
ayan.roynaskar@gmail.com

SANTOSH KUMAR

Department of Mechanical Engineering, Indian Institute of Technology (BHU), Varanasi
Varanasi, Uttar Pradesh- 221005, India
santosh.kumar.mec@iitbhu.ac.in

Abstract: The prediction of optimized forming parameters viz. the punch force, blank holding force, forming factor, and hydrostatic pressure will contribute to cost reduction of the processed metal through curtailment in material usage and manufacturing time. This article involves modeling of symmetric and axisymmetric sheet forming and hydroforming, rubber forming and axisymmetric incremental sheet forming; followed by numerical simulation using Explicit Finite Element Analysis program in ANSYS and ABAQUS. The present results are validated with previous experimental readings to check the feasibility of simulated analysis. The comparison reveals that both the readings show sound agreement in thickness distribution and load-displacement relationship. The enhanced formability in hydroformed products has been clarified by comparing with the forming factor and thickness variation. The result shows that forming factor increases with friction coefficient; thereby clarifying the need of sufficient friction to overcome cup failure. Moreover, the developed model highlighted wrinkling phenomenon in conventional forming.

Keywords: Sheet hydroforming; Finite element; Rubber pad; Fluid pressure; Incremental sheet forming.

Introduction

Globally, the demand for metal containers is increasing at an alarming rate. However, the poor formability of conventionally deep drawn products is a limitation for some industrial applications. Radial stress is a common problem in conventional forming that may result in wrinkling and tearing in some cases [1]. Numerous non-conventional techniques have been implemented that have helped expand the industrial aspect of deep drawing process such as sheet hydroforming (SHF) [2], rubber forming, etc. Attempts are being made worldwide to debilitate cost by developing punch-less and die-less forming techniques such as incremental sheet forming (ISF) [3]. Various important process parameters such as blank holding force (BHF), punch force, forming factor (K), etc. plays a significant role in achieving sound formability and uniform thickness in the deformed product. Optimization of them by numerical simulation saves production time and cost. A large number of theoretical and experimental studies have been performed to validate the feasibility of the present model. Colgan and Monaghan [4] conducted experimental study to validate the blank thickness and load-displacement variation pertaining to the deep drawing process. They concluded that punch/die radii have the greatest effect on the thickness of the formed mild steel cup. Fereshteh and Montazeran [5] predicted the optimized forming load, friction coefficient and thickness strain variation by the use of shell 51 elements of the FEA package. Kumar and Modi [2] designed an experimental setup and performed hydroforming of square cups using constant and variable BHF techniques; thereby concluding formability enhancement in the latter technique. Abedrabbo et al. [6] carried out experimental investigations of the wrinkling behavior of 6111-T4 aluminium alloys and determined load-displacement variation at different hydrostatic pressures. Billur et al. [7] experimentally studied warm hydroforming characteristics of axisymmetric stainless steel sheets and compared with the predicted values using ARAMIS software. The behavior of titanium alloys (Alberti et al. [8]) and AZ31 magnesium alloys (Xu et al. [9]) in polyurethane rubber forming technique at different load velocities were studied and optimal process parameters and tooling geometry were determined. Yamashita et al. [10] studied numerical analysis of a rubber-based cup drawing using explicit FEA in LSDYNA3D. Gulati et al. [11] carried out experimentation, simulation and optimization of tool rotation speed, feed rate, step size and predicted optimum values for the wall angle and surface roughness in Single point incremental forming (SPIF). Simulation study of Kumar and Kumar [3] highlights increase in effective stress, strain and forming forces with time in ISF process. Simultaneous experimentation was done to investigate the strain distribution in the product. The influence of tool diameter, forming angle and sheet thickness on springback, formability and surface finish in ISF were studied [12, 13]. Development of an inverse method (Bouffioux [14]) for identifying the material parameters in SPIF process is cost-effective and increases the accuracy of tool force prediction.

From the above literature survey, it is found that there is hardly any experimental analysis of axisymmetric sheet forming and SHF. Researchers mainly considered symmetric bodies in their study though theoretical investigation of axisymmetric parts has a high potential to generate deep drawn products of desired quality and fulfill the growing demands in the global market. Therefore, it has been attempted to conduct simulation of symmetric and axisymmetric forming and optimize the principle forming parameters. Study on rubber based forming process has been conducted and validated. A theoretical study is also proposed for the SPIF of an axisymmetric SS304 sheet.

Numerical simulation using Explicit FEA program in commercially available softwares ANSYS 15.0 and ABAQUS 2016 has been carried out for the following cases: (1) Conventional sheet forming (symmetric), (2) Non-conventional SHF (symmetric), (3) Axisymmetric sheet forming and hydroforming, (4) Rubber based forming, and (5) Axisymmetric ISF, respectively.

Case 1: Simulation of Deep Drawing process (Conventional)

In this process, a punch presses against a circular blank inserted between die and blank holder. A 1 mm thick SS304 sheet metal has been considered in the present study. Discrete rigid form is used to model the punch, the die and the blank holder.

1.1. *Material properties of SS304*

- Young's modulus (E) = 200 GPa
- Poisson's ratio (μ) = 0.3
- Density = 7800 Kg/m^3
- Yield stress = 340 MPa

The important dimensions of the blank, die, punch and blank holder are shown in table 1. Quadrilateral meshing with a bias ratio of 6 has been used to simulate the symmetric sheet. The reference frame is set to Lagrangian and stress-deformation contours are obtained. From the evaluated von mises stress data and material yield stress, *K* is determined in order to predict the optimum process parameters, respectively.

Table 1. Basic geometrical parameters.

Parameters	Dimensions (mm)
Blank diameter (BD)	80
Punch diameter (PD)	50
Sheet thickness (t)	1
Punch nose radius (r_p)	4
Die diameter (DD)	54
Die corner radius (r_d)	6
Radial clearance (wc)	2

The study of the influence of die design and process parameters on *K* have been conducted, according to the recommended geometrical values highlighted in table 2 **[15]**.

Table 2. Recommended parameter values [15]

Parameters	Recommended value	
r_d	(6 to 10)t	
r_p	(3 to 4)t	6.3 mm $\leq$PD <100 mm
	(4 to 5)t	100 mm $\leq$PD<200 mm
	(5 to 7)t	200 mm $\leq$PD
wc	(1.75 to 2.25)t for steel	

In the present study, it has been proved that for a punch nose radius (r_p) which is less than 3 times the sheet thickness, the cup fails due to thinning while optimum thickness is achieved for r_p greater than 3t.

1.2. *Validation*

The current work has been juxtaposed against the experimental thickness values recorded by Colgan and Monaghan **[4]**. In order to validate the model, punch velocity of 50 mm/min and BHF of 18 KN has been used according to the input parameter values used during their experimentation. Thickness values have been computed in ANSYS and ABAQUS, respectively. The comparison of the experimental and FEA results have been shown in table 3.

Table 3. Thickness comparison.

Experimental [4] (mm)	ANSYS results (mm)	ABAQUS results (mm)
1.132	1.1386	1.13958
1.032	1.07	1.08132
0.888	0.96816	0.97112
0.83	0.837298	0.83655
0.823	0.778	0.75993
0.871	0.7972	0.78597
0.966	0.9459	0.9459
0.979	0.94891	0.95955
Avg.= **0.94013**	Avg.= **0.9355085**	Avg.= **0.93499**

It is seen that the average thickness distribution in the blank of the present model is close to the experimental results.

Optimization of principle design and process parameters i.e. r_d, r_p, wc, and friction coefficient pertaining to the deep drawing process is studied in Fig. 1. Forming factor (K) represents the load carrying capacity of the present model beyond the actual loads. It can be written as:

$$K = \frac{\text{Material yield stress}}{\text{Working stress}} \tag{1}$$

By this definition, $K>1$ indicates that the design is safe and that it is capable to support the design load without failure.
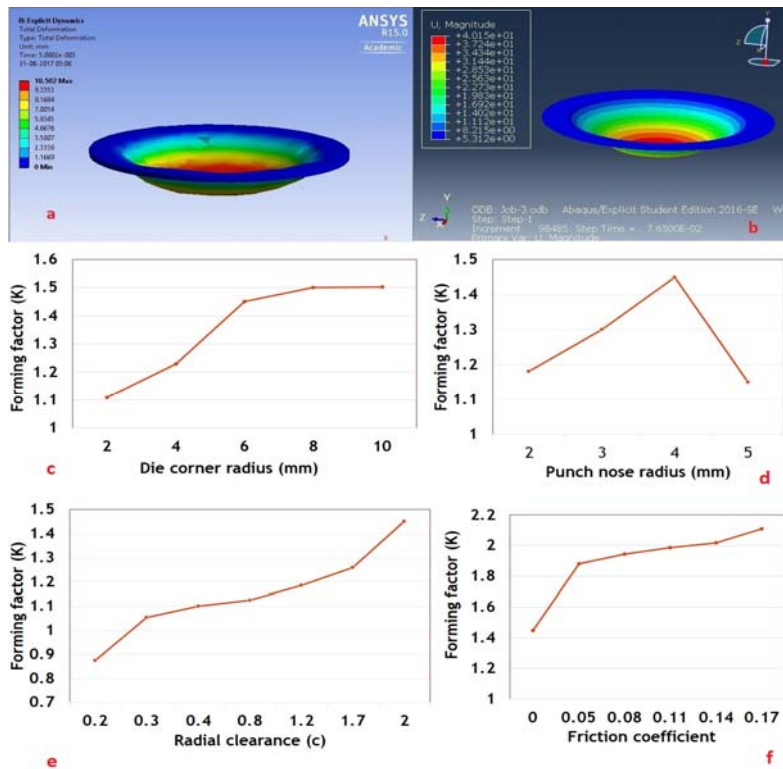
Fig. 1. Deformed result of the drawn cup in (a) ANSYS and (b) ABAQUS; Variation of K with (c) r_d, (d) r_p, (e) wc, and (f) friction coefficient

From the graphs shown in Fig. 1, the recommended values for the respective parameters can be inferred.

- r_d value in the range 6-10 mm when r_p = 4 mm and wc = 2 mm
- r_p value in the range 3-4 mm when r_d = 6 mm and wc = 2 mm
- wc value in the range 1.7-2 mm when r_p = 4 mm and r_d = 6 mm
- Friction coefficient ≥ 0.1 when r_d, r_p, and wc are 6, 4 and 2 mm

The range is found to agree with the data shown in table 2. It is seen that the K increases with the increase in r_d, r_p, wc, and friction coefficient up to a certain limit beyond which thinning will occur due to poor K value. For $wc<t$, the cup fails due to excessive thinning. Friction coefficient of 0.1 recommended.

Case 2:   Simulation of Deep Drawing process (SHF)

Unlike the conventional deep drawing process, SHF is a die-less forming process where hydrostatic pressure is applied from the opposite side of the die plate. The formability is enhanced due to fluid pressure **[16]**. As a result, the product is wrinkle free, has uniform thickness distribution throughout and is highly economical. Simulation of wrinkling behavior of SS304 has been shown using the commercial finite element package, ABAQUS as shown in Fig. 2.
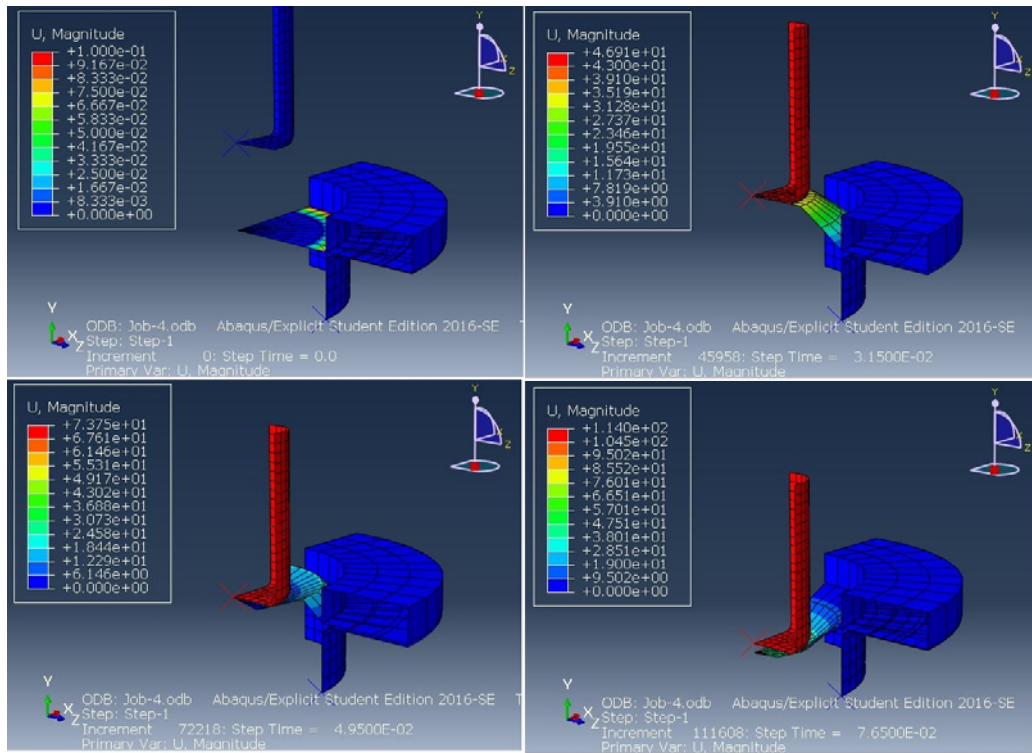
Fig. 2. Schematic of sheet hydroforming process

2.1. *Validation*

Abedrabbo et al. **[6]** carried out an experimental study of SHF at 2 MPa using AA6111-T4 as the material. In order to validate the present FEA model, experimental data has been taken from their load-displacement plot and juxtaposed with the simulated data as shown in table 4.

Table 4. Load-displacement comparison

Displacement (mm)	Experimental load (KN) [6]	FEA results (KN)
0	5	5
5	10	9
10	18	16.6
15	25	23.8
20	38	35
25	50	46.8

It can be seen that there is hardly any variation between the experimental and the present FEA readings.

2.2. *Comparison between Conventional forming and SHF*

The comparison between the conventional and SHF processes reveals wrinkle formation in the former drawn product as highlighted in Fig. 3 (a) and (b), respectively. The optimum BHF and r_d at different hydrostatic pressures has been determined for the present model. The following conclusions has been drawn from the results shown in Fig. 3.

- At a punch force of 10 KN, the maximum K value is obtained when the hydrostatic pressure is 1 MPa under a BHF of 17 KN. The K value decreases with an increase in back pressure and is minimum for the conventional process; thereby concluding formability enhancement with the application of fluid pressure [2].

- On increasing the punch force to 30 KN, the K value decreased for a back pressure of 1 MPa as compared to the one recorded for a back pressure of 2 MPa. This shows that in order to maintain the formability, increase in punch force needs to be counter balanced by a corresponding increase in back pressure.

- Maximum K value when r_d = 6-10 mm and the back pressure is 1 MPa (provided that r_p and wc are 4 and 2 mm).With increase in back pressure, a surge in the load bearing capability is observed in Fig. 3 (f).
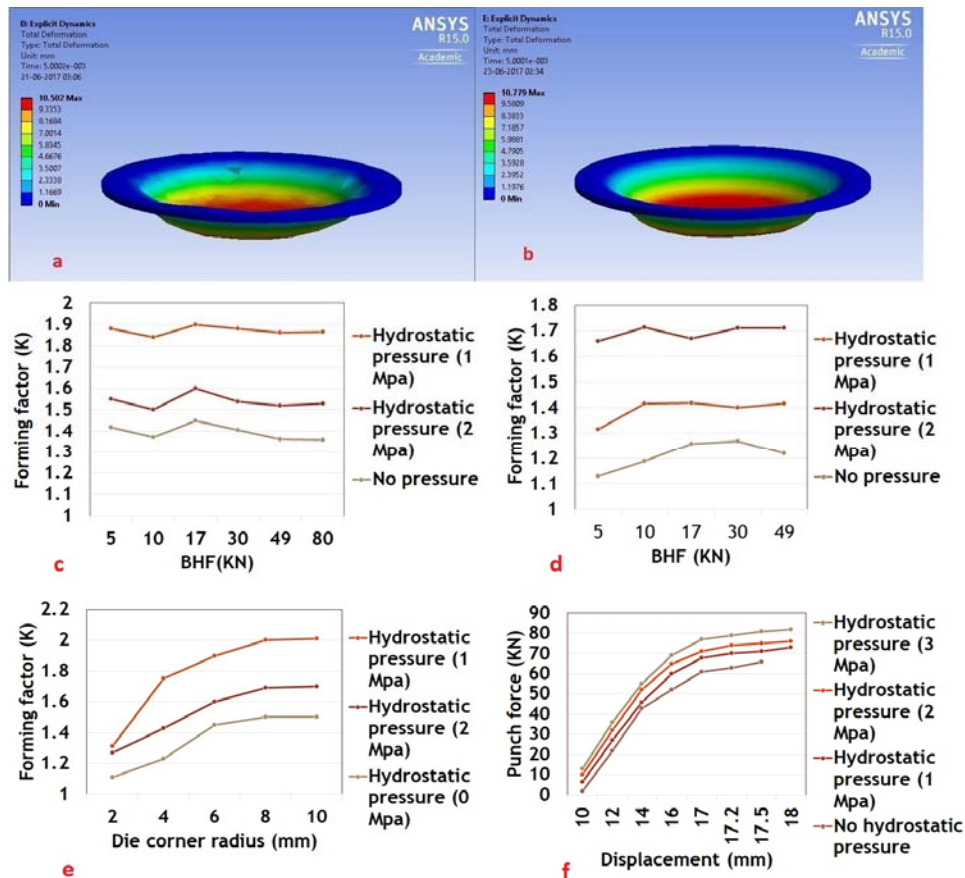
Fig. 3. (a) Conventionally formed product (b) hydroformed product; Variation of K with BHF at punch force of (c) 10 KN, (d) 30 KN

(e) Graph of K vs r_d (f) load-displacement variation

Case 3: Simulation of Axisymmetric Deep Drawing process

Earlier, our study dealt with hydroforming of symmetric blank. In this section, two axisymmetric SS304 parts have been considered where study has been performed for the 1 mm thick square blank of (80×80) mm^2 dimension, keeping the r_p, r_d and wc values constant. The important dimensions of blank, die, punch and blank holder for the square blank assembly are illustrated in table 5.

Table 5. Geometrical parameters.

Parameters	Dimensions (mm)
Blank dimensions	(80×80) mm^2
Blank thickness (t)	1 mm
Punch dimensions	(50×50) mm^2
Punch nose radius (r_p)	4 mm
Die outer dimensions	(100×100) mm^2
Die inner dimensions	(54×54) mm^2
Die corner radius (r_d)	6 mm
Radial clearance (wc)	2 mm

3.1. *Validation*

Billur et al. **[7]** highlighted his study on warm hydroforming characteristics of SS304 blank. In order to compare the FEA predictions with his experimental measurements, thickness variation of the present model is analyzed at 100 ^{o}C test temperature according to the input conditions used during experimentation. The formed parts of their experiment are compared with the simulated figure. From table 6, it is understood that the thickness of the deformed sheet is agreeable and uniform; thereby showing formability enhancement with temperature.

Table 6. Thickness variation

Distance from center (mm)	Experimental (mm) [7]	FEA result (mm)
0	0.5	0.5
5	0.51	0.49
10	0.469	0.49
15	0.51	0.5
20	0.48	0.498
25	0.46	0.5
30	0.48	0.498
35	0.458	0.497
40	0.52	0.5
45	0.54	0.51

3.2. *Simulation study*

The two axisymmetric deep drawing assemblies have been analyzed in ANSYS and the deformed results have been generated. The total deformation contour as shown in Fig. 4 (a) and (b) has been determined using a back pressure of 2 MPa. The punch force and BHF are 10 KN and 17 KN, respectively. The maximum displacement found is 10.468 mm and the maximum principle stress is 226 MPa. The comparison shows that wrinkling phenomenon is mainly prevalent in conventional forming of circular blanks. In axisymmetric study, these defects are rarely seen. The variation of K with r_d and BHF has been investigated for conventional and non-conventional process.

- Maximum K value when r_d = 8-10 mm and the back pressure is maintained at 2 MPa (provided that r_p and wc are 4 and 2 mm). With increase in hydrostatic pressure, K value decreases when r_d value is less than 6 mm.

- The maximum K is obtained when the hydrostatic pressure is maintained at 1 MPa under a BHF of 80 KN. Lower K value for conventional axisymmetric forming highlights poor formability.
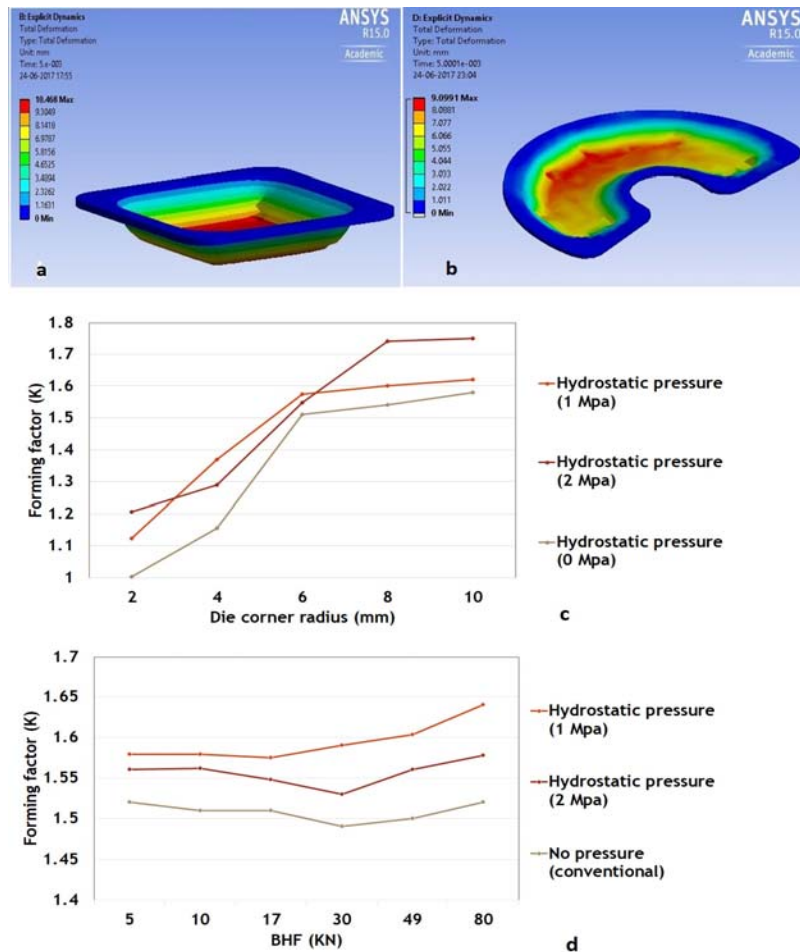
Fig. 4. (a) Final deformed product in ANSYS for (a) square blank, (b) semicircular blank; Variation of K with (c) r_d (d) BHF at punch force of 10 KN

Case 4: Simulation of Rubber forming process

Rubber based forming processes consists of a rubber pad in a rigid die. A punch presses the metallic blank against the rubber pad. The rubber exerts nearly equal pressure on all work piece surfaces due to its incompressibility. The advantage of this process is that it produces minimal spring back and profile deviation. As the punch advances, the rubber behaves almost like a hydraulic fluid. The process is die-less and thus is economical. The surface finish in the final product is hampered due to the residual wrinkles formation [9]. The diameter and thickness of the polyurethane rubber pad for the present simulation is 100 mm and 10 mm. Symmetric blank of 80 mm diameter is used.

The simulation has been done in ANSYS using explicit dynamics. The incompressible nature of polyurethane [8] justifies its use in these processes so that it can offer suitable pressure on the blank sheet without developing fracture stress. Since large strains occur in the rubber parts, it is like that contact instabilities and distortion will take place in the simulation.

4.1. *Material properties of polyurethane*

- Young's modulus (E) = 210 GPa
- Bulk modulus = 2 GPa
- Density = 1265 Kg/m^3
- Shear Modulus = 5 MPa
- Maximum tensile stress = 34.5 MPa

4.2. *Validation*

Yamashita et al. [10] conducted numerical simulation of the sheet metal drawing by Maslennikov's technique. For a single drawing operation, the comparison of the simulated and experimental displacement-time values has been found agreeable as shown in table 7.

Table 7. Displacement variation

Time	Experimental (mm) [10]	FEA result (mm)
1	0	0
2	10	10
3	15	16
4	14	15
5	12.5	12.8
6	12.5	12.6
7	12.5	13
8	12.5	12.6
9	12.5	12.6

The deformed contour shows wrinkles along the cup flanges. No stress is found to generate in the rubber. This proves that polyurethane is nearly incompressible during deformation and is capable of sustaining load **[8]**. From Fig. 5, it can be seen that:

- *K* value decreases gradually with increase in punch velocity. It is because forming stresses exceeding the yield strength of the material develops and causes cup failure. So a lower velocity between 1–10 mm/s is recommended.
- It can be seen that the blank tends to deform less for thicker rubber pads. In order to get proper deep drawn cup, optimum rubber pad thickness between 5-13 mm is necessary; otherwise the product has a shallow depth.
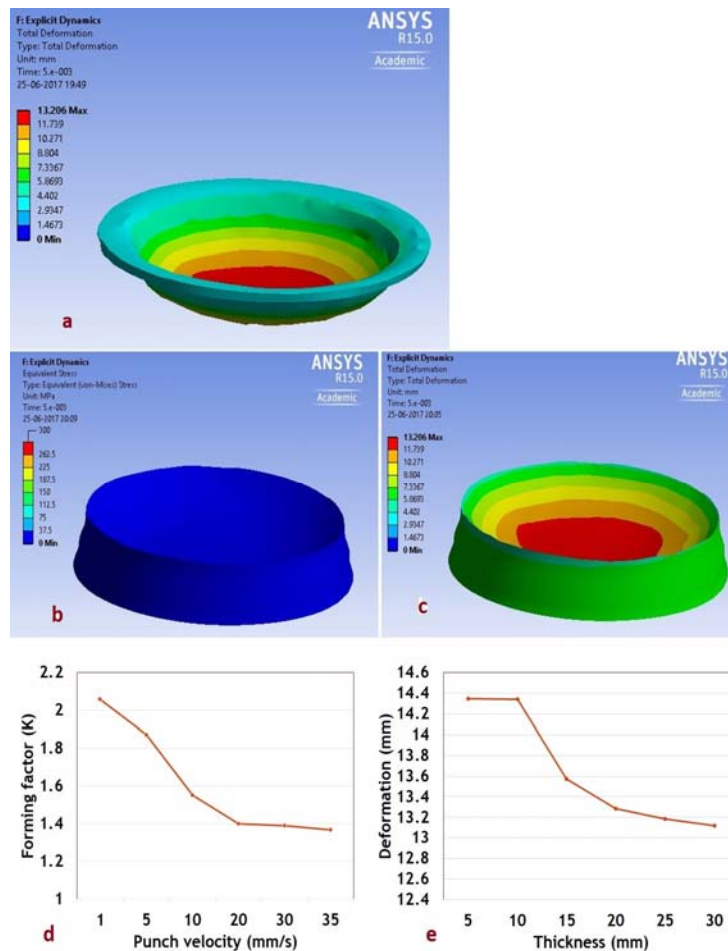
Fig. 5. (a) Deformed product; (b) stress contour of the rubber pad (c) deformation of the pad; Variation of *K* with (d) punch velocity and (e) pad thickness

Case 5: Simulation of Single point incremental forming

SPIF is a highly flexible process where a deforming tool moves in a path under control in 3D space. FEM simulation of SPIF process is a very tedious task due to the complex model and long movement of forming tool. The tool path is prepared by providing Amplitude values in dx, dy and dz direction and using a smooth step definition method in ABAQUS 16/Explicit solver. By proceeding in an incremental way, the tool is moved along the defined tool path which follows the shape of the final geometry. A square blank of (240×240) mm^2 has been studied using this process.

In order to make tool moving along predefined trajectory, tool path has been defined along X, Y and Z coordinates and a feed rate of 2000 mm/min is provided. In order to improve meshing quality, mesh size has been set to 2.

4.1. *Validation*

Singh **[12]** conducted FEA with Al5052 and obtained the stress contour result which has been compared with the present model (table 8). For validation purpose, aluminium alloy is chosen for simulation. It is seen that the stress variation in Z-direction is almost same for both the simulations.

Table 8. Stress variation

Stress (MPa) [12]	S, Mises (MPa)
3.504e+02	3.588e+02
3.214e+02	3.306e+02
2.923e+02	3.023e+02
2.633e+02	2.741e+02
2.342e+02	2.459e+02
2.051e+02	2.177e+02
1.761e+02	1.80e+02
1.470e+02	1.441e+02
1.180e+02	1.13e+02
8.891e+01	8.66e+01
5.985e+01	5.145e+01
3.080e+01	2.9e+01
1.736e+00	1.710e+00

4.2. *Simulation study*

The following discussions deals with SPIF of SS304 square blank at a tool feed rate of 2000 mm/min. The tool diameter is 5 mm with a taper angle of 4.7^o. To avoid extreme acceleration and maintain a quasi-static simulation, the deforming tool is moved by using a smooth definition method; thereby generating two shapes namely, round cup and pyramidal. It is seen that as the tool moves along its path, stress is found to increase. This is mainly due to strain hardening. The effective strain increases and gradually becomes minimum at the bottom surface **[17]**. The maximum effective strain calculated from the FEA simulation result is 0.2296 mm/mm. In case of the pyramidal cup, maximum strain (1.0 mm/mm) is formed on the walls as the deforming tool moves. This is due to the biaxial stretching at the corners of the deformed pyramidal cup. After the end of tool path, the strain decreases to a value of 0.3 mm/mm.

The feed rate of the deforming tool affects the maximum stress generation as the tool moves along its path. Both stress and strain decreases at the bottom surface. From Fig. 6 (e), the effective stress is found to increase with depth and decreases at the bottom surface **[17]**. It is seen that higher feed rate increases the stress generation along the tool path; thereby minimizing formability **[18]**. Thus, a feed rate in the range 1800-2000 mm/min is recommended. The strain is also distributed normally. In Fig. 6 (g), it can be seen that the upper undeformed surface and the bottom surface has high thickness values whereas the minimum thickness is recorded in the side walls. It is because the end point of the tool path does not reach the bottom node of the cup; thereby the thickness gradually increases after a certain depth. The thickness and nominal strains obtained in the study are within the acceptable region. Similarly, the thickness distribution along a particular circumferential path in Y direction traversed by the tool is inspected in ABAQUS. Due to the plane strain stretching of the material, the thickness is uniform in Y-direction (Fig. 6 (h)).

The same circumferential path has been considered in determining the thickness with respect to the application of hydrostatic pressures. It is found that the thickness is high and more uniform when back pressure

is applied i.e. the formability of the cup has increased in single point incremental hydroforming process as illustrated in Fig. 6 (i). Uniform stress generation in hydroforming contributes to greater thickness distribution. Flow of metal takes place due to elastoplastic deformation in the direction of forming forces and thus thickness decreases along the depth. As the tool path ends near the base of the cup, thickness is comparatively more at the bottom face of the deformed cup. The forming force increases in Z-direction (Fig. 6 (j)) while it decreases with increase in temperature [3]. A reduction up to 40% is measured between the simulated results carried out at 200 ^{o}C and 300 ^{o}C. Thus in warm conditions, formability enhancement is possible.
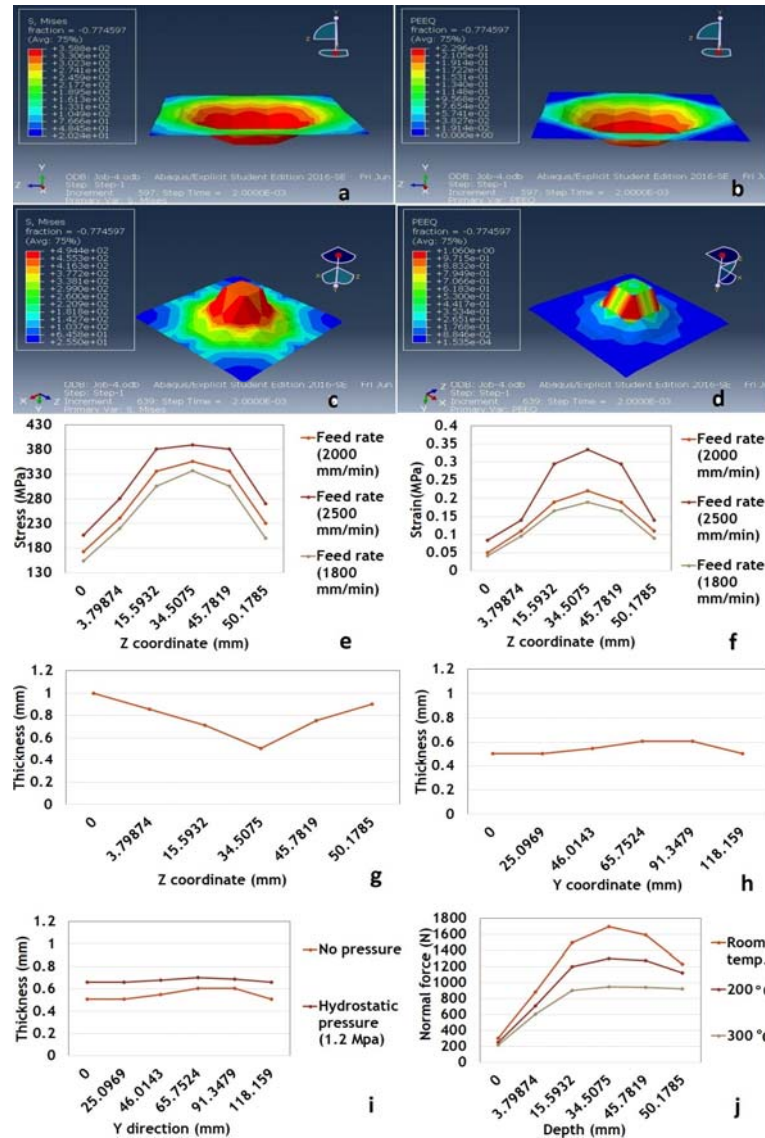
Fig. 6. (a) Stress, (b) strain contours of the round cup; (c) stress, (d) strain contours of the pyramidal cup; (e) Stress and (f) strain prediction in Z-direction; Thickness variation in (g) Z-direction (h) Y-direction; (i) Thickness variation with back pressure; (j) Force prediction

Conclusion

The effect of forming parameters in different cup drawing processes has been optimized using Explicit FEA in order to predict suitability of the product for industrial applications through saving material, production time and cost. The absence of die and punch in ISF lessens the cost and is suitable for rapid-prototyping applications. Wrinkle-free cups have been produced using SHF and SPIF. The stress and strain variation with depth of deformation has been generated in SPIF; and it has been found to be normally distributed. Lower deformation is found to occur for thicker rubber pads. In addition, the significance of higher test temperature in achieving lower forming force and uniform thickness has been emphasized.

Acknowledgements

References

[1]   Singh, C. P.; Agnihotri, G. (2015): Study of Deep Drawing Process Parameters: A Review, Int. J. Sci. Res. Publ., 5, pp. 2250–3153.
[2]   Modi, B.; Kumar, D. R. (2013): Development of a hydroforming setup for deep drawing of square cups with variable blank holding force technique, Int. J. Adv. Manuf. Technol., 66, pp. 1159–1169.
[3]   Kumar, Y.; Kumar, S. (2014): Incremental Sheet Forming (ISF), Advances in Material Forming and Joining, 5th Int. and 26th All India Manuf. Technol., Des. Res. Conf., pp. 29–46.
[4]   Colgan, M.; Monaghan, J. (2003): Deep drawing process: Analysis and experiment, J. Mater. Process. Technol., 132, pp. 35–41.
[5]   Fereshteh-Saniee, F.; Montazeran, M. H. (2003): A comparative estimation of the forming load in the deep drawing process, J. Mater. Process. Technol., 140, pp. 555–561.
[6]   Abedrabbo, N.; Zampaloni, M. A.; Pourboghrat, F. (2005): Wrinkling control in aluminum sheet hydroforming, Int. J. Mech. Sci., 47, pp. 333–358.
[7]   Koç, M.; Mahabunphachai, S.; Billur, E. (2011): Forming characteristics of austenitic stainless steel sheet alloys under warm hydroforming conditions, Int. J. Adv. Manuf. Technol., 56, pp. 97–113.
[8]   Alberti, N.; Forcellese, A.; Fratini, L.; Gabrielli, F. (1998): Sheet metal forming of titanium blanks using flexible media, CIRP Ann. Manuf. Technol., 47, pp. 217-x44.
[9]   Xu, J.; Zhou, Y.; Cui, J.; Sun, G.; Li, G. (2017): Experimental study for rubber pad forming process of AZ31 magnesium alloy sheets at warm temperature, Int. J. Adv. Manuf. Technol., 89, pp. 1079–1087.
[10] Yamashita, M.; Hattori, T.; Nishimura, N. (2007): Numerical simulation of sheet metal drawing by Maslennikov's technique, J. Mater. Process. Technol., 187–188, pp. 192–196.
[11] Gulati, V.; Aryal, A.; Katyal, P.; Goswami, A. (2016): Process Parameters Optimization in Single Point Incremental Forming, J. Inst. Eng. India Ser. C., 97(2), pp. 185–193.
[12] Singh, R.P.; Goyal, G. (2014): FEA Analysis to Study the Influence of Various Forming Parameters on Springback occurs in Single Point Incremental Forming, Int. J. Eng. Res. Appl.
[13] Gatea, S.; Ou, H.; McCartney, G.; (2016): Review on the influence of process parameters in incremental sheet forming, The Int. J. Adv. Manuf. Technol., 87, pp. 479–499.
[14]   Bouffioux, C.; Eyckens, P.; Henrard, C.; Aerens, R.; van Bael, A.; Sol, H.; Duflou, J. R.; Habraken, A. M. (2008): Identification of material parameters to predict Single Point Incremental Forming forces, Int. J. Mater. Forming, 1, pp. 1147–1150.
[15] Zein, H.; El Sherbiny, M.; Abd-Rabou, M.; El shazly, M. (2014): Thinning and spring back prediction of sheet metal in the deep drawing process, Mater. Des., 53, pp. 797–808.
[16] Forouhandeh, F.; Kumar, S.; Kumar, S. N.; Parkash, T. O. (2012): Modeling of Sheet Hydroforming of CP Titanium for semi-spherical cup shape product, Int. J. Modell. Simul. Des. Manuf. (JMSDM), 3(1-2), pp. 147–156.
[17] Ambrogio, G.; Filice, L.; Gagliardi, F. (2012): Formability of lightweight alloys by hot incremental sheet forming, Mater. Des., 34, pp. 501–508.
[18] Kim, Y. H.; Park, J. J. (2002): Effect of process parameters on formability in incremental forming of sheet metal, J. Mater. Process. Technol., 130–131, pp. 42–46.